journal

J. Am. Ceram. Soc., 78 [5] 1233–39 (1995)

Flexural Creep of Coated SiC-Fiber-Reinforced Glass-Ceramic Composites

Ellen Y. Sun*,†

Division of Engineering, Brown University, Providence, Rhode Island 02912

Steven R. Nutt*

Department of Materials Science, University of Southern California, Los Angeles, California 90089-0241

John J. Brennan*

United Technologies Research Center, East Hartford, Connecticut 06108

This study reports the flexural creep behavior of a fiber-reinforced glass-ceramic and associated changes in microstructure. SiC fibers were coated with a dual layer of SiC/BN to provide a weak interface that was stable at high temperatures. Flexural creep, creep-rupture, and creep-strain recovery experiments were conducted on composite material and barium-magnesium aluminosilicate matrix from 1000° to 1200°C. Below 1130°C, creep rates were extremely low ($\sim 10^{-9}$ s^{-1}), preventing accurate measurement of the stress dependence. Above 1130°C, creep rates were in the 10^{-8} s^{-1} range. The creep-rupture strength of the composite at 1100°C was about 75–80% of the fast fracture strength. Creep-strain recovery experiments showed recovery of up to 90% under prolonged unloading. Experimental creep results from the composite and the matrix were compared, and microstructural observations by TEM were employed to assess the effectiveness of the fiber coatings and to determine the mechanism(s) of creep deformation and damage.

I. Introduction

FIBER-REINFORCED glass-ceramic composites are being developed for high-temperature applications because of the inherent thermal and chemical stability of ceramics, the suitability of glass-ceramics to composite fabrication, and the benefits of fiber reinforcement.[1,2] Critical to the success of fiber-reinforced ceramic matrix composites (CMCs) is the presence of a "weak" fiber/matrix interface that is also stable at high temperatures.[3,4] Recently, CVD-coated fiber-reinforced glass-ceramic matrix composites have shown excellent mechanical properties and good thermal stability.[5] These composites are candidate materials for high-temperature structural applications, particularly in gas turbine engines. However, before the materials can be reliably used in structural applications at high temperatures, it is necessary to know and understand the long-term mechanical behavior, particularly the resistance to creep and fatigue. Under conditions of high temperature and applied stress, deformation, diffusion and interfacial reactions often occur, and these processes can lead to microstructural damage. Accumulation of microstructural damage degrades critical mechanical properties and eventually results in composite failure. Knowledge of the creep behavior is thus important both for material evaluation and as a basis for design of composite structures.

In recent years, research on the mechanical properties of fiber-reinforced composites has focused on fracture mechanisms and on improving room-temperature toughness. Relatively few studies have been carried out to determine the creep and creep-recovery behavior of these composites, especially at temperatures above 1000°C, the temperature range targeted for future applications. The objective of the present study is to determine the creep and creep-strain recovery behavior of a fiber-reinforced glass-ceramic composite. The creep deformation mechanisms are investigated by correlating the creep properties of the composite with those of the matrix material and the reinforcement, and also with macro- and microstructural observations of the crept samples.

II. Experimental Procedure

(1) Material

(A) Composites: The composite material selected for the present study consisted of a barium-magnesium aluminosilicate (BMAS) matrix reinforced with small-diameter SiC fibers (product designation Nicalon NLM 102, from Nippon Carbon Co., Ltd, Tokyo) coated with dual layers of BN and SiC deposited by CVD. The SiC fibers are reportedly synthesized by pyrolysis of a polycarbosilane-type precursor, resulting in nanocrystalline grains (~2 nm) and excess carbon and oxygen.[6] The BN coating was applied to the fibers by CVD at 1000°C using a proprietary precursor (3M Company, St. Paul, MN) chosen to give an approximate composition of 40 at.% B, 40 at.% N, and 20 at.% C. Carbon was deliberately added to prevent decomposition and strength degradation of fibers during the process. The oxygen content of both the SiC and BN layers was measured by Auger spectroscopy to be <3%. The tensile strength of the coated fibers was 1860 ± 255 MPa. The BMAS matrix was formulated to yield the barium osumilite composition on crystallization ($BaMg_2Al_3(Si_9Al_3O_{30})$), following the procedures described in Ref. 7. Composite panels (100 mm × 100 mm) were fabricated by hot-pressing a lay-up of 0/90° plies at 1450°C for 5 min under 6.9 MPa pressure, resulting in fiber loadings of ~50 vol%. After hot pressing, the composite panels were cut into bars and heat-treated in argon at 1200°C for 24 h in order to crystallize (or "ceram") the BMAS

A. Evans—contributing editor

Manuscript No. 193477. Received June 20, 1994; approved December 5, 1994.
Presented in part at the 18th Annual Cocoa Beach Conference and Exposition on Composites and Advanced Ceramics, Cocoa Beach, FL, January 1994 (Mechanical Behavior I—Fatigue and Creep in Ceramic/Ceramic Composites Symposium, Paper No. C-9-94F).
Supported by the Air Force Office of Scientific Research (Contract No. F49620-92-0001), by the National Science Foundation (E.Y.S.) through a Materials Research Group grant (No. DMR-9002994), and by the Office of Naval Research (S.R.N.), Contract No. N00014-91-J-1480..
*Member, American Ceramic Society.
†Current address: Oak Ridge National Laboratory, Metals and Ceramics Division, Oak Ridge, Tennessee 37831-6068.

Table I. Flexural (Three-Point) Properties of 2D BMAS/SiC/BN/Nicalon Fiber Composites (Eight Plies)

σ (MPa)						
Room temperature				High temperature		
As-pressed	Ceramed	550°C, O_2, 100 h	1200°C, air, 500 h	1100°C	1200°C	1300°C
655	675	620	510	648	565	248

matrix to the barium osumilite phase. Composites consisting of lay-ups of eight or sixteen alternating 0/90° plies were produced. The flexural and tensile properties of the eight-ply composite are listed in Tables I and II, respectively.

(B) BMAS Glass-Ceramic: The unreinforced BMAS glass-ceramic samples were fabricated by the same procedure as the composites, although slightly different processing conditions were required. Hot pressing was performed under 6.9 MPa pressure at 1050°C for 10 min, instead of at 1450°C for 5 min. This modification was required because at 1450°C in the absence of fiber reinforcement, the viscosity of the glass was too low to allow pressing without loss of material. The samples were then ceramed in argon at 1200°C for 24 h, just as the composites were. The flexural properties of the BMAS glass-ceramic are listed in Table III. The phase distribution and the grain morphology were slightly different from the composite matrix because of the different processing conditions and nucleation mechanisms. (In the composites, the fibers provide abundant nucleation sites for crystallization of the glass.) Barium osumilite was the dominant phase in the unreinforced glass-ceramic, although there was more cordierite and celsian than in the composite. Nevertheless, the glass-ceramic microstructure was sufficiently similar to the composite matrix to be useful as a control for the investigation of creep.

(2) Creep Experiments

(A) Composites: Creep experiments were performed in air using three-point and four-point bending fixtures in a dead-weight loading system. For four-point flexural creep experiments, specimens with eight 0/90° plies (~75.0 mm × 5.1 mm × 1.3 mm) and sixteen 0/90° plies (~75.0 mm × 5.1 mm × 2.7 mm) were tested. A fixture with outer and inner spans of 63.5 and 19.0 mm was used for specimens 2.7 mm thick, while for specimens 1.3 mm thick, a fixture with outer and inner spans of 40.0 and 19.0 mm was used. Creep experiments were conducted at 1000° to 1200°C under applied stresses of 100 to 670 MPa. For three-point flexural creep experiments, specimens with sixteen 0/90° plies (~75.0 mm × 5.1 mm × 2.7 mm) were tested and a fixture with an outer span of 63.5 mm was used. Creep experiments were conducted at 1100° and 1200°C with applied stresses of 100 to 670 MPa. In both cases, the deflection was measured directly at the specimen so that creep effects in the loading rollers and the load train had no influence on the measurement. The displacement of the specimen was monitored with a linear variable-differential transducer. A linear elastic analysis was employed to calculate the corresponding stress and strain values, based on the assumption that the stress gradient began and remained linear during the test.[8] All stresses reported were equal to the magnitude of the maximum outer-fiber stress. Because the analysis used is appropriate only for small deflections (~1–2% outer-fiber strain), the experimental creep strains generally were kept within this range, except for creep-rupture experiments. A plot of strain versus time was used to determine that a constant creep rate (or minimum strain rate) was reached and maintained. The stress (or the temperature) was then changed incrementally, and the procedure was repeated. Upon completion of a test, samples were cooled rapidly at an approximate rate of 50°C/min under constant load in an effort to retain the deformed microstructure.

The creep-strain recovery behavior of the composite was investigated by loading–unloading experiments. The specimens were first crept, then unloaded instantaneously and held at a stress of 10 MPa for 5 to 24 h. A single experiment usually included two or three cycles.

(B) BMAS Glass-Ceramic: Three-point flexural creep experiments were performed on the glass-ceramic samples. The dimension of the specimens was ~100.0 mm × 5.1 mm × 3.4 mm. A fixture with outer span of 63.5 mm was used. Creep experiments were conducted at 1100° to 1200°C under applied stresses of 40 to 130 MPa.

(3) Macro- and Microstructural Observations

Direct observations of the crept specimens were made using optical microscopy. The microstructures of the crept specimens were studied using analytical and high-resolution transmission electron microscopy (HRTEM). Thin foils for TEM were prepared in a conventional manner by mechanical polishing, dimpling, and ion milling. Specimens were examined using a JEOL 2010 microscope fitted with a Noran X-ray spectrometer capable of light-element detection.

III. Results and Discussion

(1) Flexural Creep Behavior

(A) Composites: A series of four-point flexural creep experiments were performed at constant temperature and incrementally increased stress to study the creep behavior of the composite over a wide range of stresses. The creep data from a typical experiment conducted at 1100°C are presented in Fig. 1. The specimen was 1.3 mm thick in this case. For each value of stress, a brief (4–5 h) period of transient creep was followed by a long period in which the creep rate was apparently constant. The creep rates during these prolonged periods were in the 10^{-9} s^{-1} range, and because the rates were so low, the stress dependence of the creep rate could not be accurately measured. For this sample, creep rupture occurred at 560 MPa. Similar creep behavior was observed for thicker specimens (2.7 mm in thickness), except that thicker specimens tended to fail at lower stress levels (~400 MPa). The fast fracture strength for thin and thick specimens was 760 and 500 MPa, respectively. Thus, both thick and thin samples failed in flexural creep at ~75–80% of the fast fracture strength.

The peculiar creep behavior presented in Fig. 1 was unexpected. To test the validity of the measured strain rates and to explore possible effects of loading geometry, three-point flexural creep experiments were conducted under similar conditions. The results from three-point bending tests were consistent with those from four-point tests. The strain–time curves were similar in shape and the measured creep rates were also in the

Table II. Elevated-Temperature Tensile Properties of 2D BMAS/SiC/BN/Nicalon Fiber Composites (Eight Plies)

Temperature (°C)	UTS (MPa)	PL (MPa)	*E* (GPa)	ε_f (%)
1100	300	61	69	0.78
1200	294	28	62	0.88

Table III. Flexural (Three-Point) Properties of the BMAS Glass-Ceramic

Temperature	MOR (MPa)	*E* (GPa)	ε_f (%)
RT	137	100	0.14
1100°C	115	93	0.12

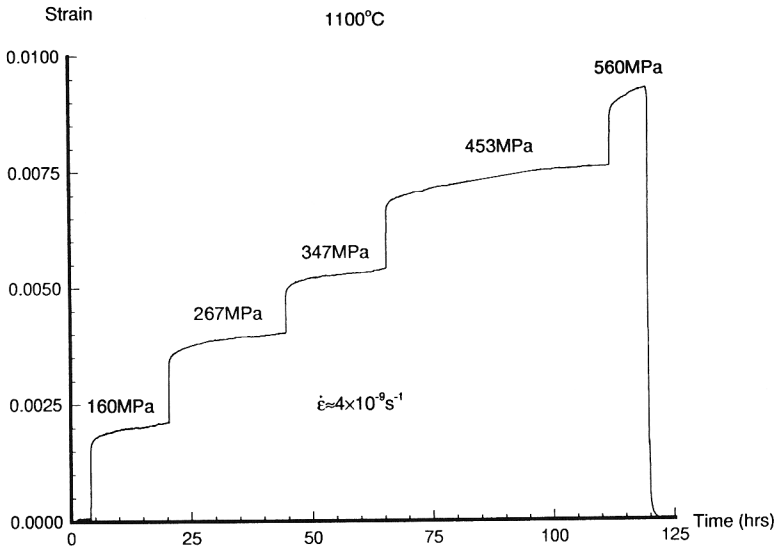

Fig. 1. Strain vs time curve of a 1.3-mm-thick specimen subjected to different stress levels at 1100°C (four-point).

10^{-9} s^{-1} range. The specimens, which were 2.7 mm thick, typically failed at ~400 MPa, just as in the four-point flexure experiments. In addition to flexural creep experiments, a tensile creep experiment was conducted in air at 1100°C under an applied stress of 103 MPa.[9] The specimen survived the 266-h test and the steady-state creep rate also was in the 10^{-9} s^{-1} range. Thus, the results from the four-point flexural creep experiments were deemed reliable.

The effect of temperature on creep rate was also investigated. Figure 2 shows the result of an experiment conducted under a constant stress of 250 MPa, periodically increasing the temperature in 30°C increments. The specimen was held for at least 24 h at each temperature level. From 1000° to 1130°C, the nominally constant creep rates were all on the order of 10^{-9} s^{-1}, while creep rupture occurred quickly above 1160°C at this stress level (250 MPa). An attempt to determine an activation energy for creep from an Arrhenius plot of log (ε)–log (1/*T*) was inconclusive because the creep rates were so low that differences between them were undetectable. However, there was clearly an effect of temperature that became apparent above ~1150°C. For example, at 1200°C, the steady-state creep rates of the composites were in the 10^{-8} s^{-1} range, an order of magnitude larger than those at 1100°C. Furthermore, the creep-rupture strength at 1200°C was only half of that at 1100°C and 45% of the corresponding fast fracture strength. These results indicate a critical temperature between 1130° and 1160°C, above which the flexural creep properties of the composite degrade significantly.

(B) BMAS Glass-Ceramic: The BMAS glass-ceramic was extremely brittle and exhibited negligible strain-to-failure in flexural creep experiments. Upon loading, a constant strain rate was obtained after a period of transient deformation. The constant strain rates were in the range of 10^{-9} s^{-1} at all stress levels from 40 to 115 MPa. At ~130 MPa, the samples failed catastrophically. By fixing the applied stress and incrementally increasing the temperature from 1100° to 1200°C, the softening temperature of the BMAS glass-ceramic was found to be ~1140°C.

The creep deformation mechanisms of the composite were studied by correlating the creep properties with those of the matrix material and the reinforcement. The tensile creep behavior of the SiC fibers at high temperatures was first investigated by Simon and Bunsell.[10] Using the same SiC fiber (NLM 102 Nicalon), they found that there existed a temperature-dependent threshold stress for creep in the 1100–1300°C temperature range. Below the threshold stress, the creep rates were lower than 10^{-8} s^{-1}, while above the threshold, the creep rates were in the range of 10^{-8} s^{-1}. The threshold stresses for tensile creep at 1100° and 1200°C were 600 and 50 MPa, respectively. Comparing their data with the results presented here, it appears that the creep behavior of the composite is controlled by the creep response of the SiC fibers. For example, at 1100°C, the creep-rupture strength of the composite was below the threshold stress for fiber creep, and presumably the SiC fibers did not undergo appreciable creep. Most if not all of the deformation that occurred in the fibers was elastic, resulting in composites with creep rates comparable to the fibers (~10^{-9} s^{-1}). On the other hand, most of the stress levels investigated at 1200°C were above the threshold stress (50 MPa), and the composite creep rates were comparable to those of the fibers alone (~10^{-8} s^{-1}). The difference in the reported threshold stress for fiber creep at 1100° and 1200°C indicates that the fibers are less resistant to creep at 1200°C. This phenomenon, plus the fact that the observed softening temperature of the BMAS glass-ceramic was ~1140°C, resulted in degradation of the composite creep properties at 1200°C.

Creep behavior of composites similar to those studied in the present work has been reported in the literature, and comparisons provide useful insights. For example, flexural and tensile creep experiments have been conducted on calcium aluminosilicate (CAS) composites reinforced with 0° and 0/90° SiC fibers, resulting in transient creep behavior (decelerating creep rates) for all stress levels employed.[11] Unlike the composites used in the present study, however, the fibers were uncoated, and the test temperature was slightly higher (1200°C).[11–13] During creep deformation, abnormal grain growth reportedly occurred in the SiC fibers, initiating at the interface and advancing radially inward. If a diffusional creep mechanism is assumed, an increase in the average fiber grain size should reduce the creep rate of the fibers, contributing to the transient decrease observed in the creep rate of the composite. Recent work has revealed that microstructural changes such as grain growth in embedded fibers are stimulated by diffusion of oxygen and/or other matrix species from the matrix.[14] However, in the present study, abnormal grain growth was prevented by the fiber coatings, which effectively prevented diffusion across the interface. As a result, the fiber microstructures were stable for long-term exposures up to 1200°C (Section III(4)). Thus, the differences in creep response between the CAS composites and the BMAS composites studied here can be attributed partly to the dynamic changes in fiber microstructure that occurred in the former material.[11] Multiple processes may be occurring during the initial period of primary creep. The weak BN coating applied to the fibers in this study may allow stresses to redistribute efficiently during

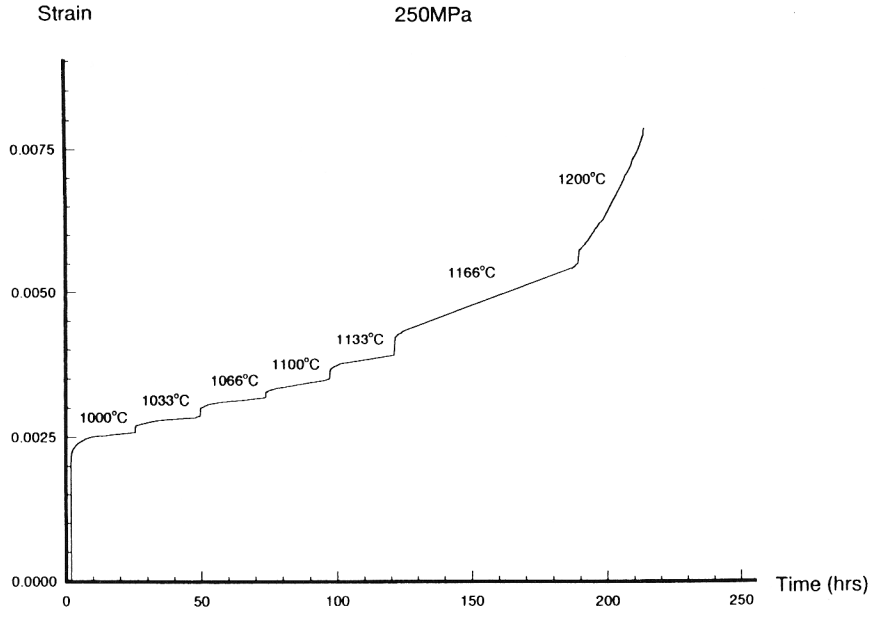

Fig. 2. Strain vs time curve of a creep experiment performed with incrementally increased temperature and constant stress level (four-point).

initial loading, leading to a constant creep rate after a relatively short period (4–5 h) of transient creep. In addition, provided the stress and temperature are sufficient, matrix flow can permit the fibers to straighten upon loading.

(2) Creep-Strain Recovery Behavior of the Composites

The creep-strain recovery behavior of a composite provides an indication of the amount of recoverable deformation introduced during a loading period, and indicates how a simple loading history of practical relevance influences the accumulated creep strain. A sample time–strain curve for two loading–unloading periods is shown in Fig. 3. During loading, the total deformation consists of an instantaneous deformation (ε_{in}) and the creep deformation (ε_{cr}). During unloading, the deformation recovered instantaneously is $\varepsilon_{in,R}$, while the (time-dependent) creep-strain recovery is $\varepsilon_{cr,R}$. The creep-strain recovery ratio R_{cr} has been used to quantify the amount of creep-strain recovery

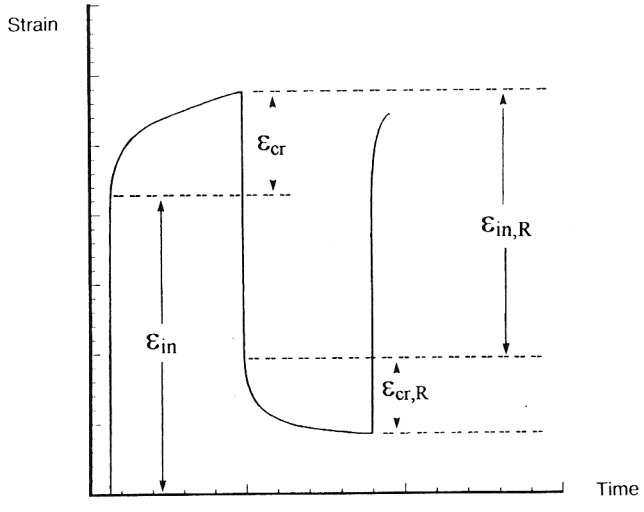

Fig. 3. Definition of some variables used to characterize the creep deformation and the strain recovery during loading–unloading experiments.[15]

that occurs during unloading. R_{cr} is defined as the creep strain recovered during a particular unloading cycle divided by the creep strain for the cycle.[15]

$$R_{cr} = \varepsilon_{cr,R}/\varepsilon_{cr} \quad (1)$$

The creep and strain recovery behavior of the BMAS composite was studied through loading–unloading experiments. Figure 4 shows the results of a typical creep-recovery experiment involving three cycles with increasing loads for each cycle. (The specimen was 2.7 mm thick and typically failed at about 400 MPa.) For the first cycle, the instantaneous deformation (ε_{in}) upon loading was larger than the strain recovered upon unloading ($\varepsilon_{in,R} + \varepsilon_{cr,R}$), implying that permanent deformation occurred during loading. The permanent deformation was caused primarily by matrix cracking and crack propagation along the fiber/matrix interface, because both the stress and strain levels (222 MPa and ~0.40%) were well above the failure strength and the failure strain of the BMAS glass-ceramic (~110 MPa and 0.13%). The creep-strain recovery ratio was about 55% for the first two cycles (unloaded for 5.6 h), and 70% for the third cycle, for which the unloading period was 20 h. In recent creep recovery experiments on similar composites, Wu and Holmes reported a 49% creep-strain recovery ratio for 0/90° SiC-fiber-reinforced CAS composites during tensile creep at 1200°C in argon.[12] Figure 5 shows the creep and strain recovery for three cycles using identical loads but different unloading periods. The creep-strain recovery ratios were different for the three cycles. For the first cycle, which had the shortest unloading period, R_{cr} was 50%. For the second cycle, the unloading period was nearly 3 times as long, and R_{cr} was 58%. This recovery ratio was similar to the recovery observed in Fig. 4 for the same applied stress (222 MPa). The third cycle involved a longer recovery period, and the measured recovery ratio was 91%.

The large creep-strain recovery observed in this composite system derives from several factors, including the creep properties of the constituents, the interfacial bonding, and the fiber distribution. For example, at 1100°C, the stress applied to the composite generally was below the threshold stress for fiber creep. Consequently, the SiC fibers deformed elastically while the matrix underwent creep. Upon unloading, elastic contraction of the fibers supplied a driving force for recovery. Because the temperature of the composite was maintained after

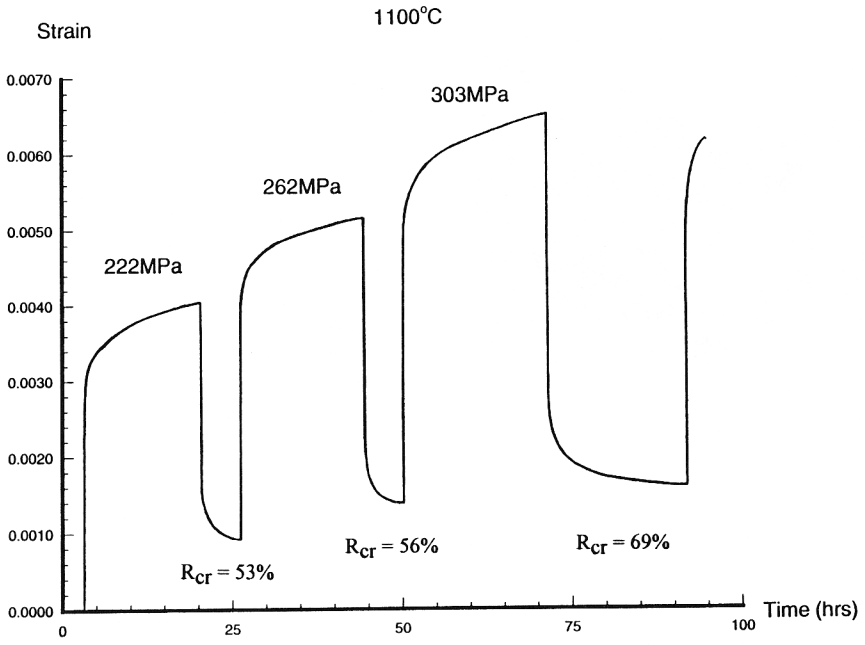

Fig. 4. Creep and strain recovery (four-point), with increasing loads for each cycle.

unloading, the fibers and the matrix relaxed, resulting in anelastic strain recovery of the composite. The recovery process was also affected by the degree of interfacial debonding that, in turn, controlled the load transfer between the fibers and the matrix. In this composite system, the BN layer provided a weakly bonded interface that also achieved effective load transfer, reducing the time needed to reach stress equilibrium between the fibers and the matrix. Holmes and Wu recently reported that significantly more strain recovery could be obtained from 0/90° composites than from unidirectional composites.[16] They concluded that the 90° (transverse) fibers provided significant resistance to axial creep deformation through lateral constraint. Thus, in the present study, residual stresses in the transverse direction should also contribute to the driving force for axial contraction upon unloading.[16] However, large strain recovery is only obtained when the applied stress during loading is low or moderate. If the stress level is close to the failure strength, extensive microstructural damage is generally introduced during the loading period. Such damage results in permanent strain that cannot be completely recovered during unloading. This can be shown by comparing the R_{cr} value of the third cycle in these two cases. For an applied stress of 303 MPa, or ~75% of the ultimate strength, only 69% of the creep strain was recovered after a 20-h unloading period, while for 222 MPa applied stress (~55% of the ultimate strength), 91% recovery was obtained after a 25-h unloading.

(3) Failure Features of the Composites

Microscopic examination of the creep-ruptured specimens revealed the distribution of damage in creep-rupture samples. Failure consistently occurred under the load pins during both four-point and three-point creep-rupture experiments. Figure 6 shows that beneath the loading points, transverse cracking and delamination cracking initiated in the 90° plies and propagated

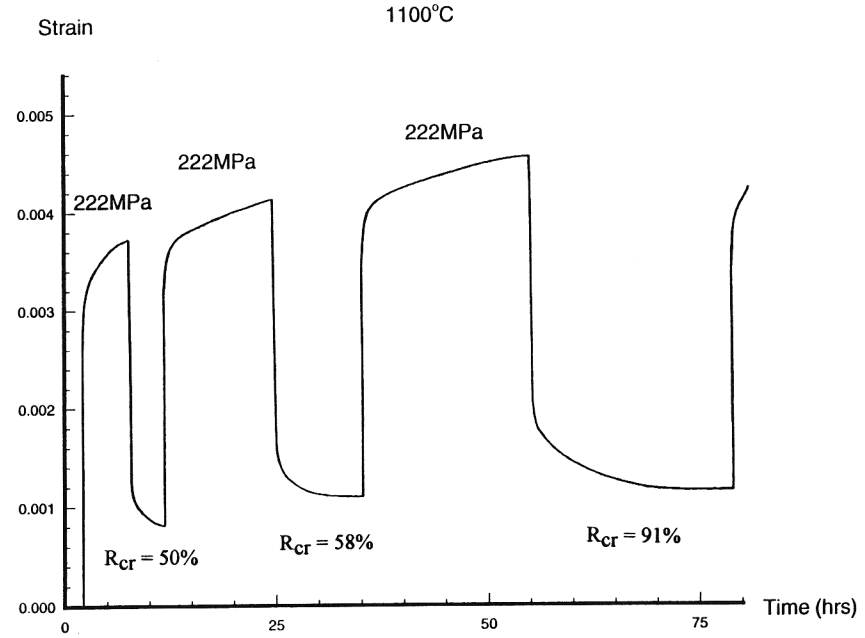

Fig. 5. Creep and strain recovery (four-point), with same loads for each cycle.

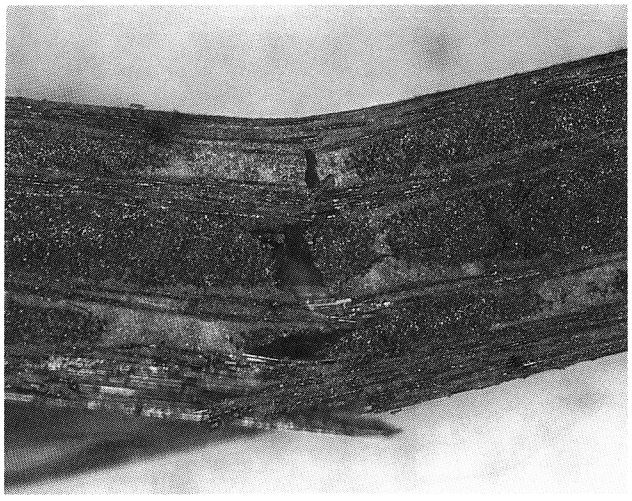

Fig. 6. Failure occurred at the loading points during creep-rupture experiment.

through the matrix into the 0° plies, resulting in fiber/matrix debonding. The composite eventually failed by fiber rupture with extensive fiber pull-out in the 0° plies. The stress concentration under the loading pins became progressively severe as damage accumulated, although our results indicate that extensive fiber rupture occurred only at the highest stress levels.

Composite failure under three-point loading involved formation of a hinge under the loading pin. At 1200°C, the creep-rupture strength of the composite was ~240 MPa, although hinge formation was observed at lower stress levels (212 MPa). The profile of a typical creep-rupture sample is shown in Fig. 7(a). Fiber buckling on the compression side of the sample was often observed in the top ply. A similar specimen crept at 1200°C under 184 MPa applied stress was uniformly bent with no hinge formation under the load pin, as shown in Fig. 7(b). In general, hinge formation did not occur until the applied stress approached the ultimate strength of the composite, leading to the conclusion that at stress levels lower than ~70% of the creep-rupture strength, the aforementioned linear elastic analysis could be applied to obtain valid flexural stress and strain values.

(4) TEM Observations of Composites after Creep Tests

The microstructure of the crept specimens was examined by transmission electron microscopy. Oxidation was generally confined to the near-surface region and the reacted layer was less than 30 μm thick. No major changes were observed in the sample interiors (beneath the near-surface region). Figure 8 shows a typical interface region after creep at 1100°C. Both the BN coating and the SiC overlayer are intact and show no evidence of change from the pretested condition. Likewise, the fiber shows no evidence of grain growth or reaction with the matrix or coating. The only change apparent in such images is the formation of subtle dual sublayers at the fiber/BN interface, evident as light and dark strips. These nanoscale layers were carbon-rich (fiber side) and silica-rich (BN side), respectively, and were produced by a carbon-condensed solid-state oxidation reaction.[17] Occasionally, slight coarsening of the BN layer occurred because of matrix element diffusion or liquid infiltration, possibly through cracks in the SiC overlayer.[17] Analysis of SAD patterns and EDS spectra indicated that neither the microstructure nor the composition had changed significantly in the SiC fiber, the BN coating, the SiC coating, or the matrix during creep at 1100°C. These observations indicate that the composite microstructure was stable under the stress–temperature conditions employed.

IV. Conclusions

The flexural creep and creep-rupture behavior of dual-coated fiber-reinforced glass-ceramic composites was investigated. At temperatures up to 1130°C, the constant creep rates were in the range of 10^{-9} s^{-1}, while at 1200°C, the constant creep rates were an order of magnitude larger. At 1100°C, the composite failed in flexural creep at ~75–80% of the fast fracture strength.

The 0/90° fiber-reinforced composites exhibited large creep-strain recovery, indicating that the creep deformation of the composites was viscoelastic. Furthermore, the results suggest that creep strains can be totally recovered after long-term heat treatment at high temperatures and under zero-load conditions, provided that the applied stress is sufficiently low to prevent extensive microstructural damage during initial loading and subsequent creep.

The dual SiC/BN coating applied to the SiC fibers provided an effective barrier to reaction and diffusion, resulting in composites that were microstructurally stable under long-term

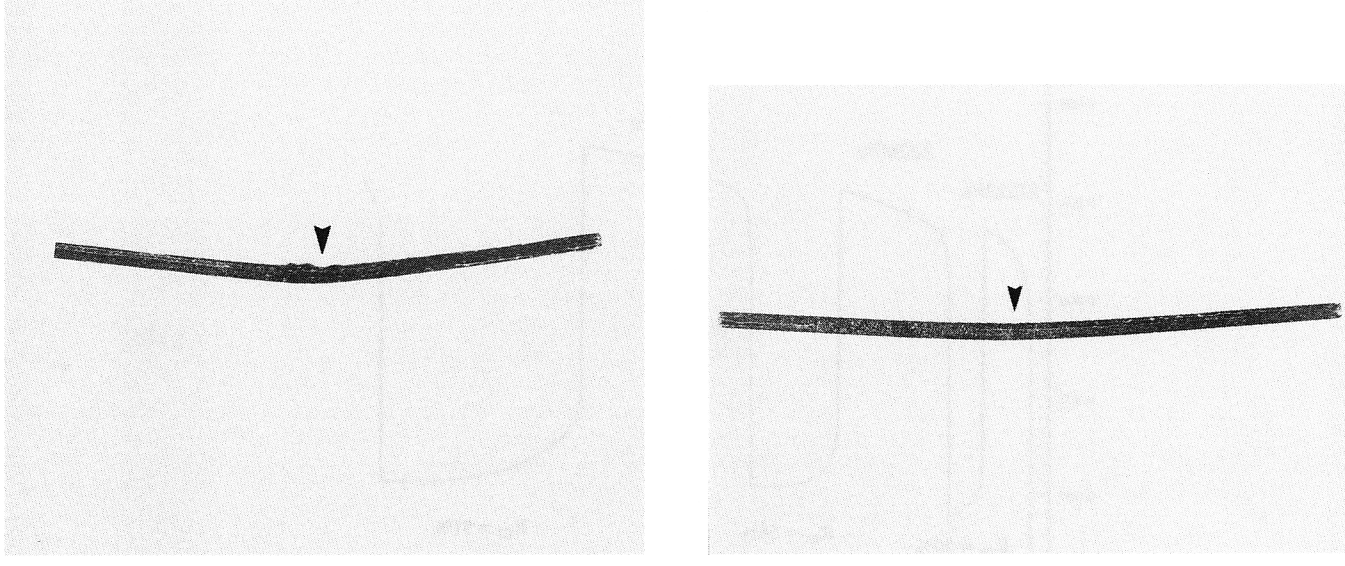

Fig. 7. (a) Profile of a specimen creep ruptured at 212 MPa (1200°C, three-point). Notice hinge formed under the loading pin. (b) Profile of a specimen crept at 184 MPa without failure. No hinge formed.

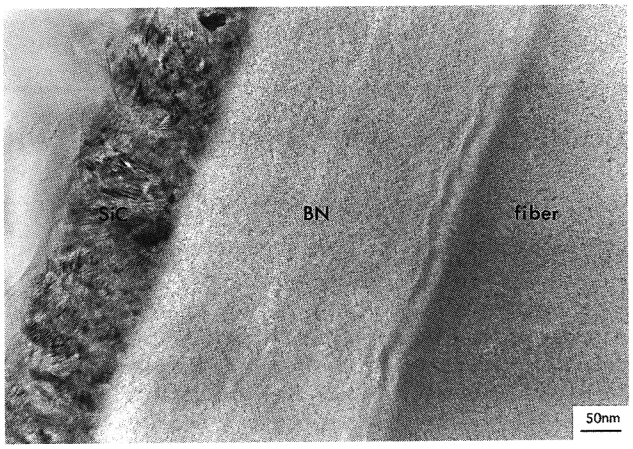

Fig. 8. Interfacial region in crept composite (1100°C, four-point).

exposure to high temperatures and stresses. In addition, the BN coating has proved to provide the desired weak interfacial bond between the fibers and the matrix. Under low and moderate applied stress, this interfacial layer allows stress redistribution to occur efficiently. During initial loading, stress redistribution leads to steady-state creep after a brief transient, while during prolonged unloading, it results in large strain recovery. On the other hand, when the applied stress is close to the ultimate strength of the material, the BN coating allows debonding to occur, resulting in extensive fiber pull-out. These energy-absorbing processes contribute to the high toughness of the composite, as reported previously.[5] The results described here lead to the conclusion that the dual coating of fibers constitutes a valid approach to the design of interfaces in continuous fiber-reinforced composites, resulting in a combination of high toughness, strength and creep resistance.

An additional outcome of the present work concerns the experimental technique. Tensile creep experiments provide important information about composite behavior, although there are usually substantial technical difficulties associated with the experiments, as well as high costs. Flexural creep experiments, on the other hand, are intrinsically problematic because of the more complex stress state, but are attractive because of the simplicity of the testing procedure and sample preparation. For the stress–temperature conditions employed in the present study, both loading methods yielded extremely low strain rates that were difficult to measure accurately. Improved extensometry would be valuable to future investigations of fiber-reinforced ceramics. While experiments could easily be conducted at higher temperatures to achieve larger strain rates, the kinetics for oxidation of the fiber and coatings are also much more rapid, and the fiber is also more susceptible to recrystallization. Consequently, the microstructure rapidly becomes unstable at extremely high temperatures. Creep experiments in controlled (nonoxidizing) atmosphere are currently being planned to evaluate the effect of oxidation on creep behavior.

Acknowledgments: We would like to thank Mr. Jim O'Kelly of 3M for coating the Nicalon fibers used in the study, Mr. Stan Kustra of UTRC and Mr. Gary Linsey of Pratt and Whitney for the composite flexural and tensile testing, respectively, and Dr. Alexander Pechenik of the Air Force Office of Scientific Research for sponsorship of this program.

References

[1]K. M. Prewo and J. J. Brennan, "High Strength Silicon Carbide Fiber-Reinforced Glass Matrix Composites," *J. Mater. Sci.*, **15**, 463–68 (1980).

[2]K. M. Prewo and J. J. Brennan, "Silicon Carbide Fiber Reinforced Glass-Ceramic Matrix Composites Exhibiting High Strength and Toughness," *J. Mater. Sci.*, **17**, 2371–83 (1982).

[3]J. J. Brennan, "Interfacial Characterization of Glass and Glass-Ceramic Matrix/Nicalon SiC Fiber Composites"; pp. 546–60 in *Materials Science Research*, Vol. 20. Plenum Press, New York, 1986.

[4]R. F. Cooper and K. Chyung, "Structure and Chemistry of Fibre-Matrix Interfaces in SiC Fibre-Reinforced Glass-Ceramic Composites: An Electron Microscopy Study," *J. Mater. Sci.*, **22**, 3148–60 (1987).

[5]J. J. Brennan, B. Allen, S. R. Nutt, and Y. Sun, "Interfacial Studies of Coated Fiber Reinforced Glass-Ceramic Matrix Composites," Annual Rept. No. R92-970150-1 on AFOSR Contract F49620-92-C-0001, November 30, 1992.

[6]S. Yajima, K. Okamura, T. Matsuzawa, J. Hasegawa, and T. Shishido, "Anomalous Characteristics of the Microcrystalline State of SiC Fibers," *Nature (London)*, **279**, 706–707 (1979).

[7]K. M. Prewo, J. J. Brennan, and G. K. Layden, "Fiber Reinforced Glasses and Glass-Ceramics for High Performance Applications," *Am. Ceram. Soc. Bull.*, **65** [2] 305–13, 322 (1986).

[8]E. M. Passmore, R. H. Duff, and T. Vasilo, "Creep of Dense, Polycrystalline Magnesium Oxide," *J. Am. Ceram. Soc.*, **49** [11] 594–600 (1966).

[9]J. J. Brennan, S. R. Nutt, and E. Y. Sun, "Interfacial Studies of Coated Fiber Reinforced Glass-Ceramic Matrix Composites," Annual Rept. No. R93-970150-2 on AFOSR Contract F49620-92-C-0001, November 30, 1993.

[10]G. Simon and A. R. Bunsell, "Creep Behaviour and Structure Characterization at High Temperatures of Nicalon SiC Fibers," *J. Mater. Sci.*, **19**, 3658–70 (1984).

[11]C. H. Weber, J. P. A. Lofvander, and A. G. Evans, "Creep Anisotropy of a Continuous-Fiber-Reinforced Silicon Carbide/Calcium Aluminosilicate Composite," *J. Am. Ceram. Soc.*, **77** [7] 1745–52 (1994).

[12]X. Wu and J. W. Holmes, "Tensile Creep and Creep-Strain Recovery Behavior of Silicon Carbide Fiber/Calcium Aluminosilicate Matrix Ceramic Composite," *J. Am. Ceram. Soc.*, **76** [10] 2695–700 (1993).

[13]X. Wu and J. W. Holmes, "Static and Cyclic Creep Behavior of a SiC-Fiber Glass-Ceramic Matrix Composite"; unpublished work.

[14]E. Y. Sun, "Microstructure and Mechanical Properties of Coated Fiber-Reinforced Glass Ceramic Matrix Composites"; Ph.D Thesis. Brown University, Providence, RI, 1994.

[15]J. W. Holmes, Y. H. Park, and J. W. Jones, "Tensile Creep and Creep Recovery Behavior of a SiC-Fiber–Si_3N_4-Matrix Composite," *J. Am. Ceram. Soc.*, **76** [5] 1281–93 (1993).

[16]J. W. Holmes and X. Wu, "Elevated Temperature Creep Behavior of Continuous Fiber-Reinforced Ceramics"; in *Elevated Temperature Mechanical Behavior of Ceramic Matrix Composites*. Edited by S. V. Nair and K. Jakus. Butterworth-Heinemann, Stoneham, MA, in press.

[17]E. Y. Sun, S. R. Nutt, and J. J. Brennan, "Interfacial Microstructure and Chemistry of SiC/BN Dual-Coated Nicalon-Fiber-Reinforced Glass-Ceramic Matrix Composites," *J. Am. Ceram. Soc.*, **77** [5] 1329–39 (1994). □